A CDK-related kinase regulates the length and assembly of flagella in *Chlamydomonas*

Lai-Wa Tam,[1] Nedra F. Wilson,[1,2] and Paul A. Lefebvre[1]

[1]Department of Plant Biology, University of Minnesota, St. Paul, MN 55108
[2]Department of Anatomy and Cell Biology, Oklahoma State University, Center for Health Sciences, Tulsa, OK 74107

Little is known about how cells regulate the size of their organelles. In this study, we find that proper flagellar length control in *Chlamydomonas reinhardtii* requires the activity of a new member of the cyclin-dependent kinase (CDK) family, which is encoded by the *LF2* (*long flagella 2*) gene. This novel CDK contains all of the important residues that are essential for kinase activity but lacks the cyclin-binding motif PSTAIRE. Analysis of genetic lesions in a series of *lf2* mutant alleles and site-directed mutagenesis of LF2p reveals that improper flagellar length and defective flagellar assembly correlate with the extent of disruption of conserved kinase structures or residues by mutations. LF2p appears to interact with both LF1p and LF3p in the cytoplasm, as indicated by immunofluorescence localization, sucrose density gradients, cell fractionation, and yeast two-hybrid experiments. We propose that LF2p is the catalytic subunit of a regulatory kinase complex that controls flagellar length and flagellar assembly.

Introduction

Cilia and flagella are highly conserved microtubule-based organelles that perform a wide array of crucial motile and sensory functions in many types of cells (for review see Davenport and Yoder, 2005). *Chlamydomonas reinhardtii* is a unicellular green algae that has been used extensively to study ciliary/flagellar function and assembly. Each *C. reinhardtii* cell has a pair of equal length flagella whose length is tightly monitored and regulated. When cells are induced to shed their flagella, they regenerate flagella rapidly to the predeflagellation length within 90 min (Rosenbaum et al., 1969). After amputation of one of the two flagella, the remaining one shortens and waits for the other one to regrow to the same length; both then grow out to the predeflagellation length. The most striking example of the active regulation of flagellar length occurs when wild-type (WT) cells are mated to mutant cells with abnormally long flagella. Within minutes after cell fusion, the long flagella shorten to the WT length (Barsel et al., 1988). These observations demonstrate the existence of a vigorous regulatory mechanism that assesses and enforces flagellar length.

Flagella are dynamic structures that undergo continuous assembly and disassembly, mainly at their distal ends (Marshall and Rosenbaum, 2001; Song and Dentler; 2001). The steady-state length of flagella is likely to be the result of equilibrium between flagellar assembly and disassembly. A wealth of experimental evidence indicates that flagellar assembly and maintenance require intraflagellar transport (IFT), a kinesin/dynein-based transport system that involves at least two protein complexes of >17 polypeptides (Kozminski et al., 1993; Cole et al., 1998). IFT particles have been observed to associate with flagellar proteins and preassembled complexes (Qin et al., 2004) and to move at defined rates up and down the flagella (Kozminski et al., 1993; Iomini et al., 2001; Dentler, 2005). Recent studies indicate that IFT is involved in the transport of signaling molecules (Qin et al., 2005; Wang et al., 2006) and in Hedgehog signaling in mouse primary cilia (Huangfu et al., 2003). The compartmentalization of IFT particles can also be modulated in response to flagellar adhesion during mating in *C. reinhardtii* (Wang et al., 2006).

Because IFT is essential for flagellar assembly, it is a likely target of regulation for controlling the length of flagella. One model for length control proposes that the length of flagella is governed by intrinsic properties of IFT that determine the extent of flagellar assembly by balancing rates of assembly and disassembly (Marshall and Rosenbaum, 2001). Genetic studies demonstrate that flagellar length is regulated by specific protein products (McVittie, 1972; Barsel et al., 1988; Asleson and Lefebvre, 1998). There are four genetic loci (*LF1* (*long flagella 1*), *LF2*, *LF3*, and *LF4*) at which mutations result in abnormally

Figure 1. **Flagellar phenotype of the *lf2-6* mutant.** (A–C) DIC images of WT cells with pairs of equal length flagella ∼13–14 μm long (A), an *lf2-3* cell with long flagella ∼21 μm in length (B), and *lf2-6* cells with unequal length flagella and stumpy flagella that have distal swollen tips (C; arrows). (D) *lf2-6* cells were unable to regrow their flagella beyond a short stump even 5 h after flagellar amputation. (E and F) In EM thin sections, short aggregates of IFT-like particles (arrows) were found filling the space between the flagellar membrane and microtubules in these distal swellings. Bars (D), 10 μm; (E and F) 100 nm. (G) A histogram showing the total length of each pair of flagella in 50 *lf2-6* cells. The length of the longer flagella was stacked on top of that of the shorter flagella.
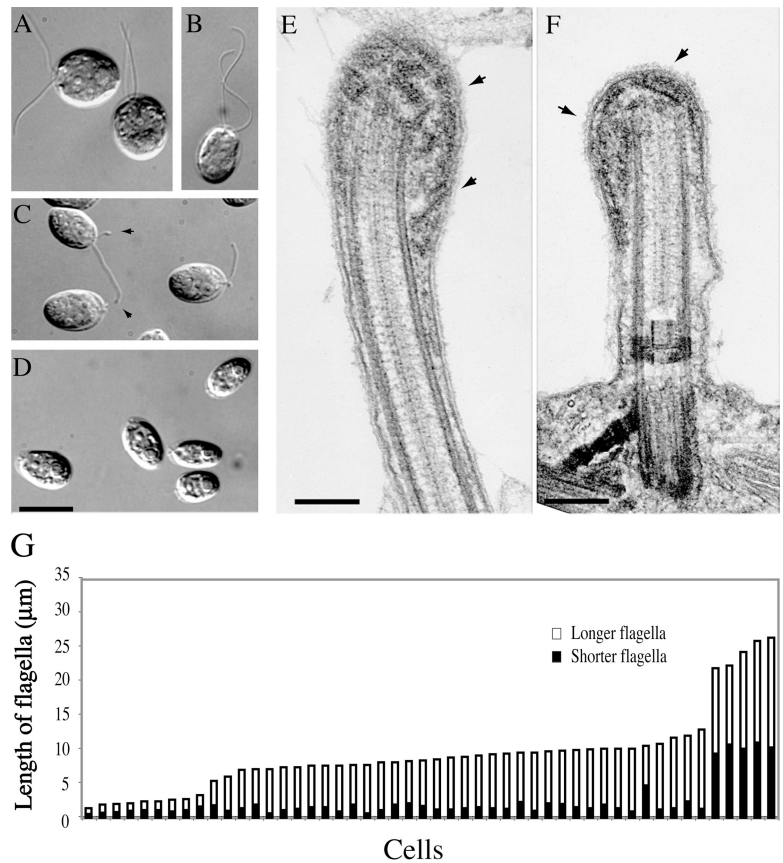
long flagella, often two to three times the normal length (McVittie, 1972; Barsel et al., 1988; Asleson and Lefebvre, 1998). The *lf1* mutant has very long flagella and regrows flagella very slowly after deflagellation. Five mutant alleles of *LF2* have been identified, and they cause varying degrees of excessive flagellar length and defective flagellar regeneration. Four previously described *lf3* mutant alleles cause the assembly of long flagella, but they can regenerate flagella normally. Recently, we described two new null mutations at *LF3* that confer a distinct unequal length flagella phenotype; the two flagella are different in lengths on most mutant cells (Tam et al., 2003). The null mutants also regenerate flagella very slowly and have prominent swellings at the distal ends of their flagella that are filled with IFT-like particles. About a dozen *lf4* mutants, which are isolated after DNA insertional mutagenesis, have very long flagella but can regrow flagella with WT kinetics after deflagellation. The gene products of three of these *LF* genes have been identified. *LF1* and *LF3* encode novel proteins of unknown function (Tam et al., 2003; Nguyen et al., 2005). *LF4* encodes a MAPK (Berman et al., 2003), providing the first evidence that protein kinase pathways are involved in flagellar length control. Recent studies also implicate glycogen synthase kinase 3, an aurora kinase, and an NIMA-related kinase in the regulation of flagellar assembly and disassembly (Pan et al., 2004; Wilson and Lefebvre, 2004; Bradley and Quarmby, 2005).

Similar mechanisms for regulating the length of cilia/flagella may exist in other organisms. For example, in *Leishmania*, the length of flagella can be shortened or increased by the overexpression or deletion of a MAPK (Bengs et al., 2005). In sea urchin blastula, cilia at the apical tuft are two to three times longer than cilia present on the rest of the embryo (Burns, 1973). In mammals, motile cilia within the same organ can be different in length depending on their location (Clary-Meinesz et al., 1997), and the length of primary cilia varies with the diameter of bile ducts (Huang et al., 2006). Perturbation of ciliary length has been shown to correlate with human diseases such as primary ciliary dyskinesia (Niggemann et al., 1992). Recently, it has been shown that mice with a particular form of juvenile cystic kidney disease have kidneys with abnormally long primary cilia (Smith et al., 2006).

In this study, we cloned *LF2* and identified its gene product as a new member of the cyclin-dependent kinase (CDK) family. CDKs have attracted intense research interest because many of them play essential roles in cell cycle progression (Morgan, 1997). In addition, CDK5 performs multiple important functions in terminally differentiated neuronal cells (Smith and Tsai, 2002). In the present study, we identify a new function for this class of kinases in regulating the size and development of an organelle. Although a close homologue of LF2p has not been identified in other organisms, several CDK-related kinases of unknown functions are highly expressed in the testis, in which germ cells are differentiating into flagellated sperm cells (Besset et al., 1999; Wohlbold et al., 2006), raising the possibility that these kinases may be the counterparts of LF2p in regulating flagellar length in higher organisms. The current study will inspire a new direction for exploring additional roles of CDKs in nondividing cells.

Results

Phenotype of the new *lf2-6* allele

C. reinhardtii cells have a pair of equal length flagella that never exceed 16 μm (Fig. 1 A). Cells containing any of the five previously identified *lf2* mutant alleles assemble extra-long flagella up to 30 μm (Fig. 1 B). Using DNA insertional mutagenesis, we have identified a new *lf2* mutant allele (*lf2-6*) whose flagellar length defect is very similar to that of the two null mutants of *LF3* (Tam et al., 2003). Although some *lf2-6* cells had flagella longer than 16 μm, most of the cells possessed stumpy or unequal length flagella (Fig. 1 C). The length of both flagella on each cell in a population of *lf2-6* cells was measured, and the majority of cells had a very short flagellum (<2 μm) and a longer flagellum (Fig. 1 G). Moreover, there was an obvious defect in the morphology of the mutant flagella: instead of having a tapered shape, the distal ends of all flagella, whatever their lengths, were swollen (Fig. 1 C, arrows). Examination of these flagella by thin-section EM revealed the accumulation of IFT-like particles at these distal flagellar bulbs (Fig. 1, E and F). Western blot analysis of flagella isolated from WT and *lf2-6* cells also revealed the overaccumulation of IFT proteins in the mutant flagella (unpublished data).

WT cells can regenerate their flagella rapidly and synchronously after they shed or resorb their flagella, reaching full length by 90 min after flagellar amputation. Several of the *lf2* alleles with a long flagella phenotype are unable to regrow their flagella after deflagellation, or they regenerate only very slowly (Barsel et al., 1988). The *lf2-6* mutant showed the most severe defect in flagellar regeneration. All of the cells were unable to grow flagella beyond a short stump of ≤1 μm (Fig. 1 D) even hours after flagellar excision.

LF2 encodes a CDK-related kinase

The tagged *lf2-6* mutant enabled us to identify genomic DNA clones that rescued the mutant phenotype upon transformation. A 7.5-kb XhoI–XhoI fragment containing a predicted CDK gene was able to complement the mutant phenotype upon transformation into *lf2-6* cells (Fig. 2 A). By combining EST sequences with RT-PCR and 5′ rapid amplification of cDNA ends (RACE) analysis, we were able to obtain a complete 2,244-bp cDNA sequence for *LF2* (genomic and cDNA sequences are available from GenBank/EMBL/DDBJ under accession nos. DQ994241 and DQ994242). When cloned into a *C. reinhardtii* gene expression cassette, the 1.1-kb coding region of this putative cDNA rescued the *lf2-6* mutation by transformation.

The predicted *LF2* gene encodes a protein of 354 aa with a calculated mass of 37,546. The N-terminal 300 aa include the 11 subdomains that are characteristic of all serine/threonine kinases (Fig. 2 B). BLAST searches indicated that LF2p is most homologous to members of the CDK family. The percentages of identity/similarity to rat CDK2, CDK4, CDK5, and CDK7 are 40/58%, 37/53%, 34/53%, and 39/53%, respectively. LF2p is most similar (47% identity and 61% similarity) to rat PNQARLE, a CDK-related kinase of unknown function (Fig. 2 B). In addition to the overall sequence homology, PNQARLE and LF2p both have a C-terminal extension that is absent in many other CDKs.
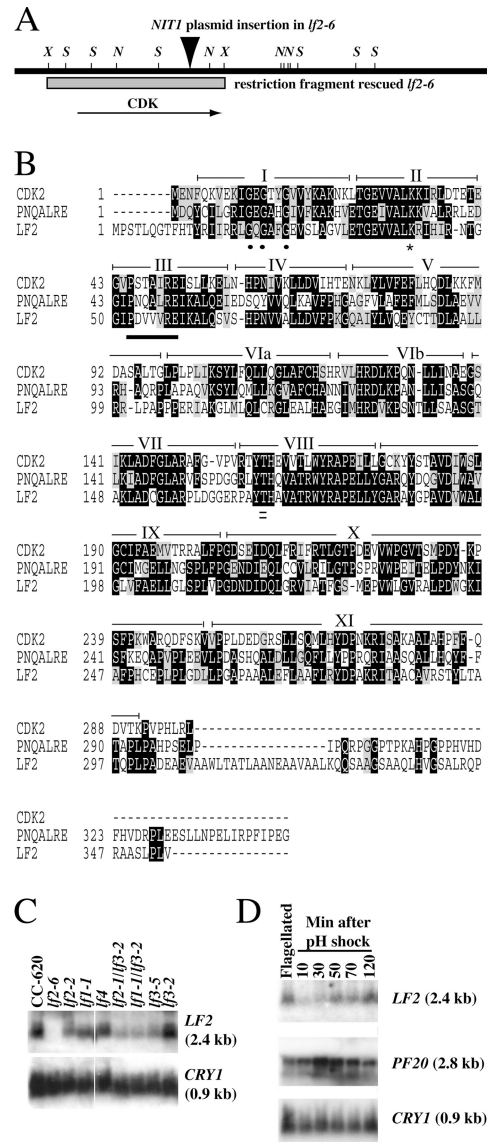

Figure 2. **Structure, ClustalW multiple alignment, and RNA analysis of the *LF2* gene.** (A) Restriction map of the genomic region around the site of insertion in *lf2-6*. The restriction sites XhoI (X), SmaI (S), and NotI (N) are shown. (B) *C. reinhardtii* LF2p is compared with a rat CDK2 and a rat PNQALRE (GenBank/EMBL/DDBJ accession no. Q63699 and Q4KM34). Identical and similar amino acids are shaded in black and gray, respectively. The 11 subdomains characteristic of serine/threonine kinases are delineated. Glycine (black dots) in the GXGXXG motif for ATP binding, the invariant lysine (asterisk) conserved in all functional kinases, residues corresponding to the cyclin-binding PSTAIRE motif (underlined), and the threonine (double underlined) that has to be phosphorylated for full activation of many CDKs are noted. (C and D) 25 μg of total RNA isolated from WT (CC-620) and various *lf* mutant strains at different times after pH-induced deflagellation in WT cells was size fractionated on formaldehyde agarose gels and transferred to nylon membranes. The blots were hybridized successively to a PCR probe spanning nucleotides 602–900 of the *LF2* cDNA sequence, a genomic DNA probe of *PF20* encoding a protein in the axonemal central pair, and a DNA probe from *CRY1* (encodes ribosomal S14 protein) for loading controls.

LF2p contains all of the aa known to be critical for the catalytic activity of CDK kinases, including the glycine-rich loop (GXGXXG) for ATP binding in subdomain I and the invariant lysine (position 41) for phosphotransfer in subdomain II (Fig. 2 B).

In CDK2, phosphorylation of threonine at position 14 and tyrosine at position 15 within the glycine-rich loop inhibits its activity, whereas phosphorylation of threonine at position 160 within subdomain VIII activates the kinase (Morgan, 1997). LF2p lacks the threonine and tyrosine residues in the glycine-rich loop but retains the second threonine at position 168 (Fig. 2 B). Another feature of many CDKs is the α helix (subdomain III) containing the PSTAIRE motif required for cyclin binding. Cyclins expressed at various phases of the cell cycle regulate the level and activity of CDKs (Morgan, 1997). In LF2p, a unique sequence, PDVVVRE, replaces the PSTAIRE motif, indicating that LF2p probably does not interact with cyclins and, therefore, is classified as a CDK-related kinase.

RNA analysis of LF2

Expression of the *LF2* transcript in WT and various *lf* mutant cells was analyzed on RNA blots with a DNA hybridization probe from the predicted *LF2* coding region (Fig. 2 C). A 2.4-kb RNA was detected in WT cells (CC-620) as well as in long flagella mutants *lf1-1*, *lf2-2*, *lf3-2*, and *lf4*. The *LF2* transcript was not observed in the insertional mutant *lf2-6*, strongly suggesting that *lf2-6* is a null mutant. Interestingly, the *LF2* transcript level was substantially reduced in *lf3-5*, a null mutant of *LF3*, and in two double *lf* mutants, *lf1-1 lf3-2* and *lf2-1 lf3-2*, all with unequal length flagella. This observation shows that accumulation of the *LF2* RNA could be affected by null mutations in *LF3* or by double mutations of *LF1*, *LF2*, or *LF3*.

During flagellar regeneration, the transcript levels for flagellar proteins increase rapidly and transiently (Lefebvre et al., 1980). We examined the transcript level of *LF2* at various times after flagellar amputation in WT cells. In contrast to flagellar gene transcripts such as *PF20*, whose level increased during flagellar regeneration, the amount of *LF2* RNA appeared to decrease early during regeneration (Fig. 2 D), suggesting that LF2p is unlikely to be a flagellar protein.

Expression of epitope-tagged LF2p

Attempts to generate antibodies to bacterially expressed LF2 protein or to synthetic peptides were unsuccessful. Therefore, we tagged the cDNA construct with the HA epitope so that LF2p could be detected with a commercially available HA antibody. The HA-tagged construct rescued the *lf2* mutants as efficiently as the untagged version. When total proteins from several rescued strains were analyzed on Western blots using an HA antibody, a cluster of at least three protein bands migrating at ~42 kD was detected only in cells rescued with the HA-tagged construct (Fig. 3 A, top and bottom). The amount of the higher mol wt isoforms decreased, whereas the level of the smallest mol wt isoform increased when cell extracts containing the HA-tagged proteins were incubated at 37°C (Fig. 3 B, no PPI). However, this size change was inhibited if phosphatase inhibitors were included during the preparation of cell extracts (Fig. 3 B, +PPI). These results may be explained by the presence of phosphatase activity in cell extracts and because the higher mol wt forms of LF2p are phosphorylated forms of LF2p.
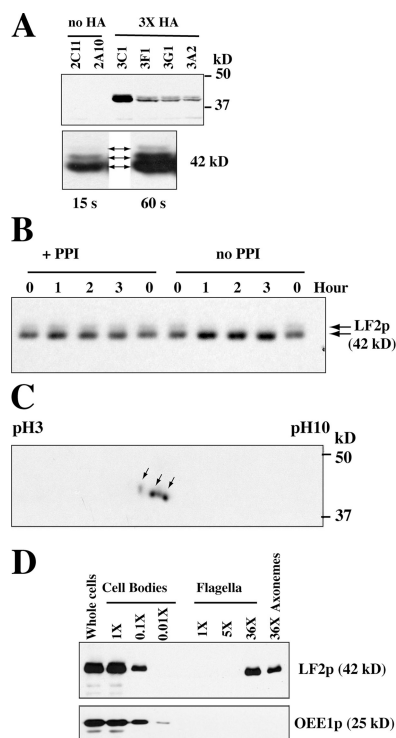

Figure 3. **Western blot analysis of HA-tagged LF2 protein.** (A) Total protein from two strains (2C11 and 2A10) rescued with the untagged *LF2* construct and four strains (3C1, 3F1, 3G1, and 3A2) rescued with the HA-tagged *LF2* construct were size fractionated on an SDS-PAGE gel, transferred to a PVDF filter, and detected with an HA antibody (top). A cluster of bands migrating at ~42 kD were observed only with cells expressing the tagged construct. When total cell protein from 3G1 was resolved on a longer gel (bottom; 15- and 60-s exposures), at least three isoforms were visible (arrows). (B) Soluble proteins were extracted from 3F1 cells by freezing/thawing twice in a buffer either with (+PPI) or without phosphatase inhibitors (no PPI). Cell extracts were incubated at 37°C for the amount of time indicated and analyzed on a Western blot. (C) 2D gel analysis of LF2p. Arrows point to the three major isoforms of HA-LF2p. (D) Comparison of the amount of LF2p in whole cells, cell bodies, flagella, and axonemes. Flagellar or axonemal protein from 10^6 ($1\times$), 5×10^6 ($5\times$), and 3.6×10^7 ($36\times$) cells were compared with 10^6 whole cells and cell body proteins from 10^6 ($1\times$), 10^5 ($0.1\times$), and 10^4 ($0.01\times$) cells. The same blot was reacted with an antibody to a chloroplast protein, OEE1, to determine the amount of cell body contamination in the flagella preparations.

The LF2p isoforms were resolved by 2D gel electrophoresis. The two higher mol wt forms of LF2p were focused at a lower pH (Fig. 3 C), as would be expected if they are phosphorylated forms of LF2p. pI values of the isoforms were estimated by their positions on the first dimension. On three separate gels, estimated pI values between the largest and smallest isoforms were within 0.6 of each other, which can be accounted for by the possible addition of one to three phosphate groups to the protein.

Because *LF2* plays a regulatory role in flagellar assembly, we examined the distribution of LF2p in the cell body and in the flagella. The majority of LF2p was detected in the cell bodies, although a very small amount was consistently observed in flagella (Fig. 3 D). The presence of LF2p in these flagellar samples could not be explained by the presence of contaminating cell bodies in these samples because very little staining with antibodies to a chloroplast protein, OEE1
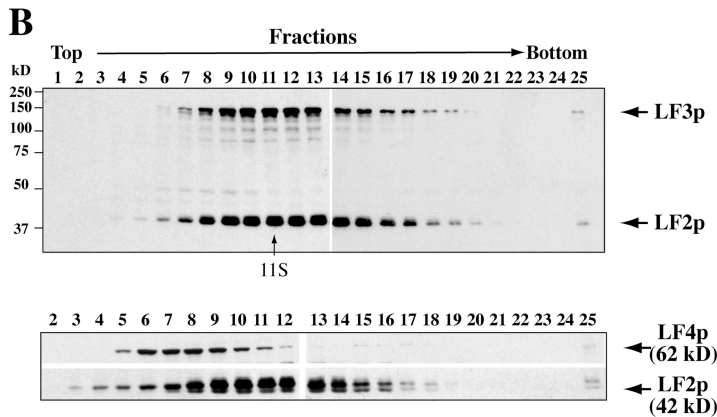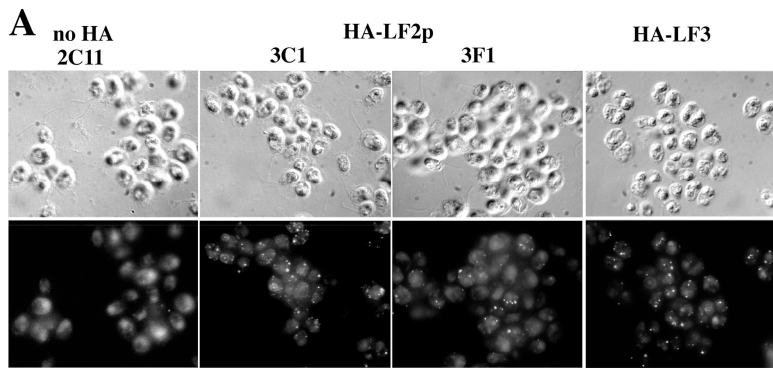
822   JCB • VOLUME 176 • NUMBER 6 • 2007

Figure 4. LF2p localized with LF3p. (A) Immunofluorescence studies localized HA-LF2p and HA-LF3p to punctate spots inside the cells. Top panels are DIC images, and bottom panels are immunostaining with the HA antibody and an Alexa-Fluor488 secondary antibody. (B) LF2p comigrated closely with LF3p in sucrose density gradients. Cell extracts from strains expressing either HA-LF2p or HA-LF3p were mixed and loaded on a 5–20% sucrose density gradient for parallel analysis. Samples were collected from top to bottom and analyzed using SDS-PAGE and Western blots. In the bottom panel, the sedimentation of LF4p was compared with that of LF2p.

(Mayfield et al., 1987), was observed with these samples (Fig. 3 D). The amount of LF2p in flagella isolated from 3.6×10^7 cells was about the same as the amount contained in 10^5 cell bodies, indicating that ≤0.3% of LF2p was distributed in flagella (Fig. 3 D). Some of the flagellar form of LF2p was detergent insoluble and remained with the axonemal fraction after 1% NP-40 extraction. It is noteworthy that there was no difference in the relative amount of the different LF2p isoforms in flagella versus cell bodies.

LF2p localization similar to LF3p

Previous studies indicated that the protein products of *LF1* and *LF3* are predominantly localized inside the cell, probably in protein complexes (Tam et al., 2003; Nguyen et al., 2005). When cells expressing HA-LF2p or HA-LF3p were analyzed in parallel by immunofluorescence, similar punctate staining of both proteins was observed inside the cell bodies (Fig. 4 A). No flagellar staining was detectable in either case.

To test whether LF2p may form a complex with the other LF proteins, we studied the sedimentation of HA-tagged LF2p or LF3p from cell extracts on sucrose density gradients. LF2p and LF3p copurified in the same fractions, with the majority of the proteins sedimenting in fractions 9–13, around 11S (Fig. 4 B, top). Previously, we found that LF1p cosedimented with LF3p in the same sucrose density fractions (Tam et al., 2003). In contrast, when the sedimentation of LF4p was compared with LF2p in another experiment, most of the LF4p sedimented away from LF2p in fractions 6–9 (Fig. 4 B, bottom). These results suggest that LF2p may be a member of a protein complex involving LF1p and LF3p but not LF4p.

Interaction of LF2p with other LF proteins in the yeast two-hybrid system

We used a GAL4 yeast two-hybrid system to test for direct interactions among LF proteins. A 1.1-kb cDNA of *LF1* and full-length coding regions of *LF2*, *LF3*, and *LF4* were cloned into yeast vectors, and their interaction was determined by the level of β-galactosidase activity (Table I). LF2p interacted specifically with LF3p and LF1p. Interaction between LF1p and LF3p was also detected. In contrast, LF4p did not interact with any of the three LF proteins.

Nature of genetic lesions in *lf2* mutant alleles

Five previously identified *lf2* alleles differ in the severity of their flagellar length defects and their ability to regenerate flagella after deflagellation (see description in the following two paragraphs; Barsel et al., 1988). We determined the sequences of four of the mutant alleles (Fig. 5 A) and correlated the lesions with the severity of their mutant phenotype (Fig. 5 B). In *lf2-1*, the 5′ donor site of intron 1 was changed (GT to AT), resulting in an abnormal splicing event at a position 26 bp downstream. The 26-bp addition to the mature RNA caused a shift of the reading frame, thereby introducing incorrect aa and a premature translational stop. Therefore, *lf2-1* is expected to make no protein or, at best, a nonfunctional truncated product that includes only two kinase subdomains. Although *lf2-1* cells have been reported to have long flagella, our reexamination of two available *lf2-1* strains revealed that many of these cells had unequal length flagella that have swollen distal tips similar to the null mutant phenotype of *lf2-6* cells (unpublished data).

Table I. **Yeast two-hybrid assay of LF proteins**

DNA-binding plasmid	DNA-activating plasmid	β-galactosidase
		Miller units
LF2	LF1	12.5 ± 0.1
LF2	LF3	15.8 ± 3.2
LF2	LF4	1.0 ± 0.1
LF2	SV40 T-antigen	1.5 ± 0.2
LF4	LF1	0.4 ± 0.1
LF4	LF3	0.4 ± 0.0
LF1	LF3	61.1 ± 3.2

The results were obtained from a representative experiment in which two different yeast transformants were assayed for each combination of proteins. SV40 T-antigen was used as a negative control for interaction.

lf2-1 mutant cells also did not regenerate flagella after amputation (Barsel et al., 1988).

In *lf2-2*, a nucleotide change at the 3′ acceptor site of intron 2 changed the consensus AG to TG. As a result, splicing took place 6 bp downstream at the next AG site, removing a glycine and a glutamine located in the junction between subdomains IV and V of the protein. These two residues are not well conserved among different CDKs (Fig. 2 B). *lf2-2* has the weakest mutant phenotype of all *lf2* alleles. Only 4–30% of cells displayed long flagella (16–20 μm), and flagellar regeneration was only slightly delayed in *lf2-2* relative to WT (Barsel et al., 1988; unpublished data).

In *lf2-3*, two nucleotide changes were found: one in the 5′ splice site (GT to AT) and one in the 3′ splice site (AG to AC) of intron 1. As a consequence, intron 1 was retained in the mature RNA, and 39 aa were inserted in subdomain I right after the glycine-rich loop. The insertion in *lf2-3* is expected to disrupt the structure of the protein and to affect its activity. The *lf2-3* mutant strain has a severe phenotype: >50% of cells have abnormally long flagella (Fig. 6 A), and many cells did not regenerate flagella until 2–3 h after deflagellation (Fig. 6 B). In *lf2-5*, a nonsense mutation changing the codon TGG to TGA was found. The mutant protein is predicted to contain 233 aa lacking the last kinase subdomain XI and the C-terminal tail. The function of subdomain XI and the C-terminal tail is not known, but the *lf2-5* truncated protein appears to retain partial function, as *lf2-5* has a moderate flagellar length defect and can regenerate flagella with nearly normal kinetics (Barsel et al., 1988).

Mutated LF2p failed to regulate flagellar length

Analysis of *lf2* mutants suggests that the catalytic kinase function of *LF2* is important for the regulation of flagellar length. To directly test the role of the kinase activity of LF2p in flagellar length control, we engineered specific mutations in the HA-tagged *LF2* gene construct that should affect only the catalytic activity but not the overall structure of LF2p. One change converted the invariant lysine at position 41 to an arginine (K41R), a change used routinely to create kinase-dead versions of various kinases (Snyder et al., 1985; Gibbs and Zoller, 1991). In a second construct, we converted the second glycine in the glycine-rich loop to a valine (G21V), a change that can greatly diminish
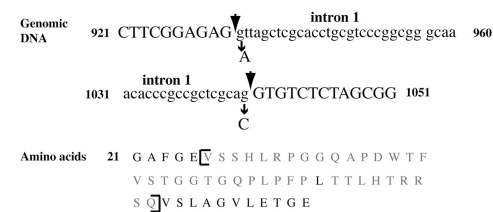

A

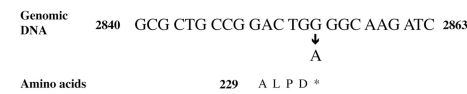**1   Intron donor site mutation in *lf2-1***

Genomic DNA 921 CTTCGGAGAG gttagctcgcacctgcgtcccggcgg gcaa 960
A

Amino acids 21 G A F G E I S S H L R P G G C L * R A Y W R R V R

2   Intron acceptor site mutation in *lf2-2*

Genomic DNA 1561 acccgcacctag GGCCAG GCCATCTACCTG 1590
T

Amino acids 75 D V F P K G·Q A I Y L

3   Intron splice site mutations in *lf2-3*

Genomic DNA 921 CTTCGGAGAG gttagctcgcacctgcgtcccggcgg gcaa 960
A

Genomic DNA 1031 acacccgccgctcgcag GTGTCTCTAGCGG 1051
C

Amino acids 21 G A F G E V S S H L R P G G Q A P D W T F
V S T G G T G Q P L P F P L T T L H T R R
S Q V S L A G V L E T G E

4   Nonsense mutation in *lf2-5*

Genomic DNA 2840 GCG CTG CCG GAC TGG GGC AAG ATC 2863
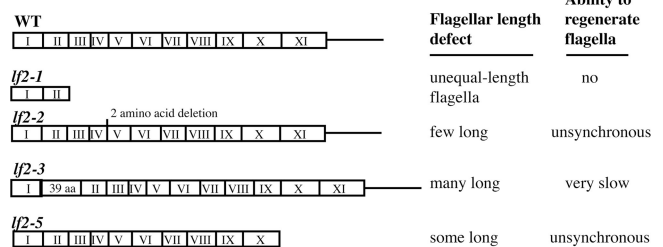A

Amino acids 229 A L P D *

B

Figure 5. **Genetic lesions in four *lf2* mutants.** (A) Nucleotide changes in the different alleles are indicated under the WT genomic sequences. Three of the mutations involve intron splice sites. The normal splice sites (arrowheads) and alternative splice sites (double arrows) are indicated. The corresponding changes in protein sequences are shown in gray. (B) Summary of the protein structure and phenotype of the mutants.

the kinase activity of the mutated enzyme (Hemmer et al., 1997). The WT construct and the two mutant constructs were introduced into the null *lf2-6* mutant by transformation to test for the effect of the mutations on the function of the protein. Although the WT construct could rescue the *lf2-6* phenotype completely, the mutant constructs could not. Nevertheless, cells expressing the mutant constructs were clearly distinguishable from *lf2-6* because many of the transformed cells assembled flagella (Fig. 6 A). Notably, >50% of cells containing the K41R construct and >20% of cells containing the G21V construct still possessed flagella longer than 16 μm (Fig. 6 A). In addition, although *lf2-6* could not regenerate flagella after deflagellation, cells harboring the mutant gene constructs were able to regrow flagella slowly (Fig. 6 B). It is noteworthy that cells transformed with the K41R construct displayed a flagellar length and regeneration phenotype almost identical to that of

the *lf2-3* mutant (Fig. 6, A and B), in which an insertion was predicted to disrupt the kinase function of the protein.

These results clearly demonstrate the importance of the kinase activity of LF2p for maintaining proper flagellar length. In contrast, the G21V and K41R constructs were able to support flagellar assembly in the null mutant background. One possible explanation for this result is that LF2p supports flagellar growth by a function independent of its kinase activity, such as facilitating the assembly of a protein complex. Alternatively, the mutated constructs may have residual kinase activity that is sufficient to support flagellar assembly but not proper length control. To distinguish these two possibilities, we combined both G21V and K41R mutations in the same *LF2* construct to further decrease the kinase activity of the protein without affecting the LF2 protein in other ways. When transformed into *lf2-6* cells, the double mutant construct was unable to rescue the null mutant. We conclude from these results that the single mutant constructs allow flagellar assembly because they retain partial kinase activity.

The protein products from six K41R and G21V transformant lines were examined by Western blot analysis. In all samples, only a single band was observed at the position of the fastest migrating isoform of LF2p (K41R transformants are shown in Fig. 6 C). The higher mol wt isoforms, which are the presumed phosphorylated proteins (Fig. 3, B and C), were missing, suggesting that LF2p kinase activity may be required directly or indirectly to phosphorylate LF2p.

Discussion

LF2 encodes a CDK-related kinase that plays multiple roles in flagellar biogenesis

In this study, we show that the *LF2* gene encodes a novel CDK-related kinase. Analysis of an allelic series of *lf2* mutants exhibiting different degrees of flagellar length and flagellar growth phenotypes has provided useful insights into the functions of *LF2*. Three of the mutants that display a long flagella phenotype—*lf2-2*, *lf2-3*, and *lf2-5*—contain mutations that are expected to produce a hypomorphic effect caused by reduced catalytic activity of the protein. The severity of the mutant phenotype in these three mutants appears to correlate with the extent of disruption in the kinase domain of the proteins. On the other hand, when LF2p is completely absent, as in the null mutant *lf2-6*, cells exhibit multiple defects: (1) a reduced ability to assemble flagella, as reflected by the high percentage of stumpy flagella cells in a population; (2) an inability to maintain an equality of length between the two flagella of a cell; (3) an inability to regenerate flagella after deflagellation; and (4) an accumulation of IFT-like particles at the distal ends of flagella, where flagellar assembly and disassembly occur. Based on these results, we conclude that LF2p plays multiple roles in flagellar assembly, including support of flagellar growth, balance of length between the two flagella of a cell, and enforcement of normal flagellar length.

Nine CDK proteins have been annotated in the *C. reinhardtii* genome (Bisova et al., 2005). LF2p, which is annotated as CDKI1, appears to have evolved to perform specific functions in
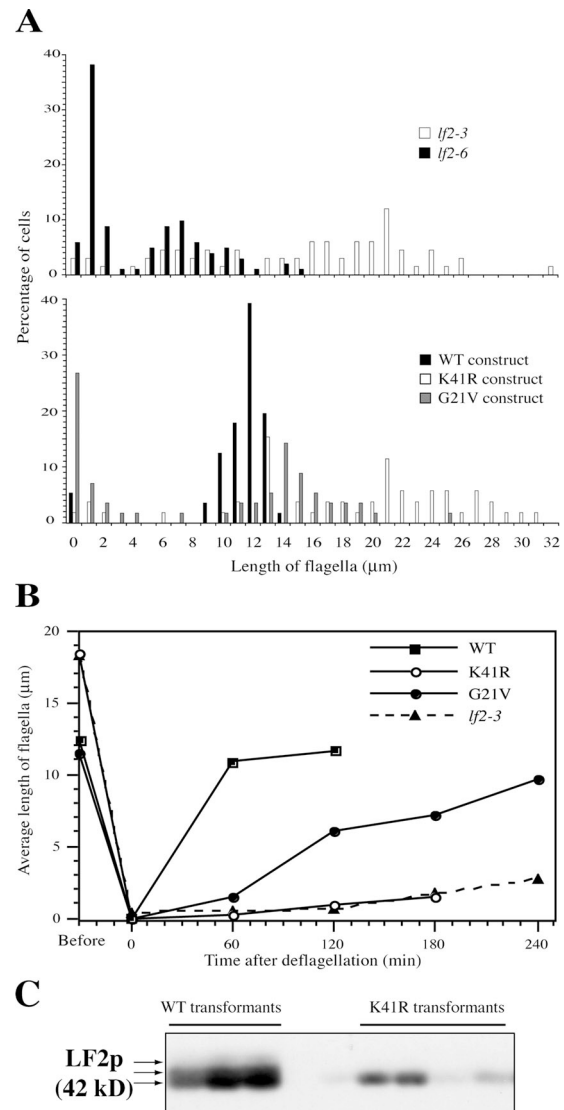

Figure 6. **Phenotype of K41R- and G21V-rescued cells.** (A) Histograms showing flagellar length distribution in populations of *lf2-3* and *lf2-6* mutant cells and *lf2-6* cells rescued with the WT construct or mutant constructs (K41R and G21V). (B) Kinetics of flagellar regeneration in WT cells, *lf2-3* mutant, and strains transformed with the mutant *LF2* constructs. Cells harboring the K41R construct showed severe retardation in flagellar regeneration similar to *lf2-3* cells. (C) Western blot analysis of transformants rescued with the WT or K41R construct. Three isoforms of LF2p were detected in WT transformants, but only the fastest migrating form of LF2p was observed in K41R transformants as well as in G21V transformants (not depicted).

flagellar assembly. Although no orthologue of LF2p can be identified in other organisms, it is most similar to the mammalian CDK-related kinase PNQALRE in sequence identity and overall structural organization. PNQALRE was first proposed to be a CDK-activating kinase that phosphorylates other CDKs (Liu et al., 2004). However, a more recent study reported that the CDK-activating activity is caused by the association of PNQALRE with CDK7 (Wohlbold et al., 2006). Interestingly, PNQALRE mRNA is most abundant in testes (Wohlbold et al., 2006), the site of assembly of sperm tail axonemes, raising the possibility that PNQALRE may play a similar role to LF2p in ciliogenesis.

LF2p kinase activity is required in vivo

Some proteins with conserved kinase domains do not require kinase activity to function (Yoshikawa et al., 2001). We used site-directed mutagenesis to test the role of LF2 kinase activity in vivo. A change at the second glycine in the highly conserved ATP-binding domain or a change in the invariant lysine in subdomain II often produces inactive protein kinases. Both mutant proteins fail to maintain flagellar length control, indicating that the kinase activity of LF2p is required to enforce flagellar length. Importantly, these mutations do not completely abolish the function of LF2p because the transformed cells were able to assemble flagella. It is possible that these mutations do not totally eliminate the catalytic activity of LF2p. There is a precedent that even mutating the invariant lysine could leave residual catalytic activity in some kinases (Robinson et al., 1996), and there is at least one example of an active kinase that lacks this conserved lysine (Xu et al., 2000). When both G21V and K41R mutations were introduced in a single construct to further reduce the kinase activity of LF2p, the double mutant construct became completely nonfunctional in rescue of the mutant phenotype. Because these mutations should only affect the phosphotransfer reaction but not the structure of the protein, the kinase activity of LF2p is the only activity required to carry out its functions. In addition, it appears that a higher level of kinase activity is required for flagellar length control, whereas a lower level of kinase activity is sufficient to support flagellar growth. We are developing in vitro kinase assays to test the predictions from these experiments.

Most CDKs are phosphorylated by other kinases, and a few can phosphorylate themselves (Chao et al., 2007). For LF2p, there are at least three isoforms. The higher mol wt forms may be phosphorylated proteins, as they could be converted to the lowest mol wt form by a phosphatase-like activity in cell extracts and were focused at a lower pH on 2D gels. Interestingly, only the smallest isoform of the protein was detected in strains expressing the low activity K41R and G21V constructs, raising the possibility that LF2p may autophosphorylate or that there is a feedback loop that regulates LF2p phosphorylation.

A protein kinase complex involving LF1, LF2, and LF3 proteins

Previous genetic studies indicate that the gene products of *LF1*, *LF2*, and *LF3* may work together to regulate flagellar assembly (Barsel et al., 1988; Tam et al., 2003). Double mutants of *lf1* and any of the hypomorphic alleles of *LF2* or *LF3* produce a synthetic stumpy flagella or unequal length flagella phenotype (Barsel et al., 1988; Tam et al., 2003). Although the length defect of *lf* mutants can be complemented rapidly when these cells fuse with WT cells to form temporary dikaryons during mating, all pairwise crosses of *lf1*, *lf2*, and *lf3* alleles fail to restore their flagellar length control in dikaryons (Barsel et al., 1988), indicating that some common structure or process is defective in these mutants. The resemblance of null or hypomorphic mutants in *LF2* and *LF3* also lends support to the idea that these genes work in similar pathways.

During flagellar regeneration, the level of RNA transcript for all three *LF* genes did not increase but rather decreased transiently during the first 30 min after deflagellation (Tam et al., 2003;

Nguyen et al., 2005; this study). In addition, the RNA transcript of *LF2* was diminished in the *lf3*-null mutant and in double mutants of *lf1 lf3* and *lf2 lf3*, and a similar reduction in the RNA transcript of *LF3* has also been observed in the null mutant of *lf2* and in double *lf* mutants (Tam et al., 2003). These almost identical accumulation patterns of *LF* transcripts suggest that the expression of these three genes is coordinated.

At the protein level, the LF1, LF2, and LF3 proteins were localized by immunofluorescence to similar cytoplasmic foci, and these proteins also cosedimented on sucrose density gradients, suggesting that they may form a protein complex. Using yeast two-hybrid assays, we demonstrated the specific interaction of these proteins in vivo. Based on all of these results, we propose that LF1, LF2, and LF3 proteins work together as a protein complex in the cytoplasm, which we call the length regulatory complex (LRC) because of its role in regulating flagellar length. We hypothesize that LF2p is the catalytic subunit of the LRC, with LF1p and LF3p being the accessory proteins for activation or recruitment. Many CDKs are inactive as a monomer and require binding to cyclins for activation. All cyclins contain a conserved region of 100 aa known as the cyclin box that binds the PSTAIRE helix of CDKs (Lees and Harlow, 1993). Noncyclin binding partners also exist for CDKs. One class of noncyclin regulatory proteins is distinct from cyclins in their primary sequence but have a similar tertiary structure to cyclins. For example, p35/p25 binds and regulates the activity of CDK5, a kinase with important functions in neuronal cells (Tarricone et al., 2001). Other noncyclin regulatory proteins that bind CDKs have no structural similarity to cyclins: for example, the Ringo/Speedy proteins that interact with CDK1 and CDK2 (Nebreda, 2006), PIF-1B and PIF2 that bind to the N-terminal extension of the CDK-related kinase PFTAIRE (Rascle et al., 2003), and MAT1, a RING finger protein that can stabilize and alter the substrate specificity of a CDK7–cyclin H complex (Devault et al., 1995; Yankulov and Bentley, 1997). LF1p and LF3p are novel proteins that are distinct from cyclins, and they are likely to be new examples of noncyclin binding partners for CDKs.

Does LF4p interact with the LRC?

Previously, our laboratory identified a MAPK, LF4p, as a regulator of flagellar length (Berman et al., 2003). LF4p, unlike LF2p, does not affect flagellar assembly. Null *lf4* mutants can assemble flagella both during the cell cycle and after deflagellation (Asleson and Lefebvre, 1998). In addition, cell fractionation studies show that LF4p is enriched in flagella (Berman et al., 2003), but very little of LF1, LF2, and LF3 proteins are located in the flagella (Tam et al., 2003; Nguyen et al., 2005; this study). We do not know how LF4p localizes inside the cell because antibodies to this protein do not work for immunolocalization, but the cytoplasmic form of the LF4 protein sedimented in lighter fractions in sucrose density gradients than the other LF proteins. Previously, it was shown that *lf4* mutations can suppress the *lf1* regeneration phenotype in *lf1 lf4* double mutants, and *lf4* mutations can suppress the stumpy flagella phenotype of *lf1-1 lf2-3* double mutants to produce long flagella (Asleson and Lefebvre, 1998). However, we are doubtful that LF4p works directly downstream from the LRC because the *lf4*

mutation cannot suppress the null *lf2* or *lf3* mutant phenotype (unpublished data). Our yeast two-hybrid experiments also did not show any direct interaction of LF4p with LRC proteins. It is more likely that the *LF4* kinase pathway and LRC pathway work in parallel to regulate flagellar length, with some cross talk between them.

Targets of the LRC

CDKs have diverse roles and many phosphorylation targets (Ubersax et al., 2003). The complex phenotypes of *lf* mutants suggest that the LRC may also have multiple targets. One obvious level of regulation is RNA accumulation. We observed a decreased level of transcript accumulation for the *LF2* and *LF3* genes in the null mutants or double mutants of *LF1*, *LF2*, and *LF3* (Tam et al., 2003; this study). Many CDKs have been shown to be part of the transcriptional protein complex, to phosphorylate the C-terminal domain of the RNA polymerase large subunit, or to be part of RNA splicing complexes (for review see Loyer et al., 2005). It will be important to determine whether the LRC regulates these cellular functions.

Another possible target for the LRC is the IFT machinery. *lf* mutants, especially the null mutants, show an overaccumulation of IFT particles at the distal ends of their flagella, the major location for flagellar assembly and disassembly. A similar abnormal accumulation of IFT particles at flagellar tips occurs in mutants defective in specific IFT components (Pazour et al., 1998; Piperno et al., 1998; Hou et al., 2004; Pedersen et al., 2005). Moreover, some IFT mutants show unequal length flagella (Pazour et al., 1998; Hou et al., 2004), leading to the hypothesis that LF1, LF2, and LF3 proteins may regulate IFT (Tam et al., 2003). Dentler (2005) measured the rate of IFT particle movements on various *lf* mutant flagella and did not detect any major difference in the kinetics of retrograde or anterograde transport in *lf* mutants. Recently, Pan and Snell (2005) demonstrated that the cargo-carrying capacity of IFT particles could be modified. When flagella were induced to resorb by chemical treatment, a large amount of cargo-free IFT particles entered into the shortening flagella and carried disassembled flagellar components back to the cell. It is possible that the LRC regulates qualitative properties of IFT such as cargo loading, the unloading capacity of IFT particles, or the activation/inactivation switch between the anterograde/retrograde motors that occurs at the distal end of flagella.

Because the LRC is localized mainly in the cytoplasm, a satisfactory model must explain how IFT is modified in the cytoplasm to affect its function in flagella. The identity of the LRC as a protein kinase complex suggests that phosphorylation may be the mechanism. Little is known about how the IFT particles are assembled and transported inside the cytoplasm before they enter the flagella. Based on the similarity of domain structures between IFT proteins and the protein components of intracellular coated vesicles, it has been postulated that the IFT machinery may have originated as specialized membrane vesicles (Jekely and Arendt, 2006). There are many examples of CDKs or CDK-related kinases that phosphorylate intracellular membrane components (Lowe et al., 1998; Smith and Tsai, 2002; Kano et al., 2004; Palmer et al., 2005). It is not difficult to envision the use of a specialized protein kinase complex, the LRC, to regulate a specialized transport system for cilia and flagella.

Materials and methods

C. reinhardtii strains

WT strain (CC-620), mutant *lf2-1* (CC-803 and CC-912), *lf2-4* (CC-2288), and *lf2-5* (CC-2287) were obtained from the *Chlamydomonas* Genetics Center. *lf2-2* (cs89) and *lf2-3* (185) were laboratory strains that were previously described (Barsel et al., 1988). *lf2-6* is an insertional mutant tagged with the nitrate reductase (*NIT1*) plasmid (Tam and Lefebvre, 1993). An *arg7* mutant was crossed with *lf2-3* or *lf2-6* to create double mutant strains for transformation.

Cloning of *LF2*

DNA from *lf2-6* was cloned into a λ-bacteriophage vector using the Lambda Fix II/XhoI partial fill-in vector kit (Stratagene) according to the manufacturer's instructions and was screened with ^{32}P-labeled pUC119 DNA to identify clones containing genomic sequences flanking the integrated *NIT1* plasmid. A fragment from one of the phage clones was used to identify eight clones from a bacterial artificial chromosome (BAC) library of *C. reinhardtii* genomic DNA (available from the Clemson University Genomics Institute). Crude DNA from BAC clones was prepared by alkaline lysis. A fragment from one of the BAC clones was used as a hybridization probe to identify a 20-kb genomic clone, λ2-4, from a WT *C. reinhardtii* λ-phage library. To test for the presence of the *LF2* gene in these clones, BAC or λ-DNA was cotransformed with pArg7.8 (Debuchy et al., 1989) into *arg7* strains containing *lf2-3* or *lf2-6* mutations as described previously (Tam and Lefebvre, 1993).

The sequence of a 17-kb region around *LF2* was determined by sequencing plasmid subclones of λ2-4 using universal sequencing primers and gene-specific primers (Advanced Genetics Analysis Center, University of Minnesota). The complete cDNA sequence was obtained and verified using three different approaches: RT-PCR and 5′ RACE products, two ESTs available from the *Chlamydomonas* Genome project, and PCR products amplified from a gametic cDNA library (provided by B. Snell, University of Texas Southwestern Medical Center, Dallas, TX). PCR, 5′ RACE, RNA analysis, and quantitation were performed as described previously (Tam et al., 2003). The genetic lesions in *lf2* mutants were determined by direct sequencing of genomic PCR and RT-PCR products from the mutant alleles. No sequence change could be found in *lf2-4* (CC-2288), and it no longer displayed any mutant phenotype, suggesting that the mutation may have reverted.

Construction of *LF2* cDNA constructs

The coding region of *LF2* was amplified from a gametic cDNA library with a primer with an NdeI site (5′-CCGCATATGCCGTCGACGCTTCAAGGC-3′) and a primer with an EcoRI site (5′-GACTGAATTCTCACACGAGCGGC-AATGACG-3′) using PfuUltra polymerase (Stratagene) and was cloned into pPCR2.1 (Invitrogen). A resulting clone was digested with NdeI–EcoRI, and the 1.1-kb insert was cloned into a psaD promoter/3′ untranslated region cassette (Fischer and Rochaix, 2001) to generate the cDNA clone psaD-LF2. To add the HA epitope to psaD-LF2, the HA cassette was excised from p3XHA (Tam et al., 2003) and cloned into a unique PmlI site 16 aa before the translational stop codon. Lysine 41 and glycine 21 were mutagenized to an arginine and a valine, respectively, according to protocols from the QuikChange II XL Site-Directed Mutagenesis kit (Stratagene). All clones were sequenced to ensure that no error was introduced during the amplification or cloning processes.

Flagellar regeneration, light, and EM microscopy

Cells were induced to shed their flagella by pH shock and were grown under bright light with shaking or stirring. Cells were taken at different times, fixed with an equal volume of 2% glutaraldehyde, and examined with differential interference contrast (DIC) microscopy optics using a microscope (Diaplan; Leica) with a 100× NA 1.25 objective (Leitz). Images of cells were captured using a video camera (CCD 72; Dage-MTI, Inc.) and Image 1.59 software (Scion). Flagellar length was measured with Image J version 1.31 software (National Institutes of Health). Thin-section EM of whole cells was performed as described previously using a microscope (1200EXII; JEOL; Tam et al., 2003). All DIC and EM images were assembled using Photoshop CS2 software (Adobe).

Protein sample preparation, Western blotting, and immunofluorescence

To determine the distribution of LF2p in flagella, cells were harvested by centrifugation, resuspended in 10 mM Hepes and 5 mM MgSO4, and deflagellated by pH shock. Cell bodies were collected by low speed centrifugation. The supernatant fraction containing flagella was underlaid with 25% sucrose and centrifuged to remove the remaining cell bodies. Purified flagella were collected by centrifugation at 23,000 g. Half of the flagella was further extracted twice with 1% NP-40 in buffer to prepare axonemes. Protein concentration was determined using the Protein Assay kit (Bio-Rad Laboratories).

Whole-cell or cell body protein samples were prepared by boiling 5×10^7 cells in 0.5 ml SDS-PAGE buffer (62.5 mM Tris, pH 6.8, 5% 2-mercaptoethanol, 2% SDS, 10% glycerol, and 0.05% bromophenol blue). Flagella were boiled in SDS-PAGE buffer to a final concentration of 2 mg/ml. Soluble proteins were extracted from cells by two to three cycles of freezing/thawing and were analyzed on sucrose density gradients as described previously (Tam et al., 2003). Phosphatase inhibitors (50 mM NaF, 25 mM β-glycerophosphate, and 1 mM sodium orthovanadate) were added to the extraction buffer except when noted otherwise.

All protein samples were size fractionated by SDS-PAGE and transferred to polyvinylidene difluoride (PVDF) membranes. Primary antibodies used were a rat HA antibody (3F10; 1:1,200; Roche Biochemicals), a rabbit anti-OEE1 (1:3,000), and a rabbit antibody to LF4p (Berman et al., 2003). Secondary antibodies are an anti–rat HRP at 1:8,000 and an anti–rabbit HRP at 1:24,000 dilutions (Sigma-Aldrich). Blots were analyzed sequentially with different antibodies without stripping. ECL reagents (GE Healthcare) were used for detection.

Protein samples for 2D gel electrophoresis analysis were prepared by freezing and thawing cells in a buffer containing 40 mM Tris, pH 7.5, 1 mM EDTA, 1 mM sodium orthovanadate, and protease inhibitor (P-8340; Sigma-Aldrich). 80 μg (in 5 μl) of the soluble proteins was mixed with 10 μl of 8-M urea and 4% Triton X-100 for 1 h at RT, and 120 μl of rehydration buffer (8 M urea, 4% CHAPS, 20 mM DTT, 0.2% biolytes 3–10, and 0.001% bromophenol blue) was then added. Samples were applied to 7-cm immobilized pH gradient strips, pH 3–10 or 5–8 (Bio-Rad Laboratories), and were focused using a Protean IEF cell (Bio-Rad Laboratories) and the default slow ramp method with active rehydration for 12 h. The second dimension was run on 8% polyacrylamide gels (10×10 cm). Proteins were transferred to PVDF membranes and analyzed with the HA antibody.

Immunofluorescence was performed on methanol-fixed cells using the HA antibody at a 1:400 dilution and an AlexaFluor488 fluorochrome–conjugated secondary antibody at a 1:500 dilution (Invitrogen) according to procedures described previously (Tam et al., 2003). Images were captured on a CCD camera (CoolCam; Cool Camera Co.) and assembled using Photoshop CS2 (Adobe).

Yeast two-hybrid assay

The interaction of LF proteins was studied according to procedures detailed in the Yeast Protocols Handbook (CLONTECH Laboratories, Inc.). The full-length coding region of *LF2*, *LF3*, and *LF4* and a partial *LF1* cDNA encoding aa 1–330 were cloned into plasmid vectors pGBKT7 (GAL4 DNA-binding domain) and pGADT7 (GAL4 activation domain) and tested in the yeast strain SFY526. All LF constructs were also tested alone or in combination with control plasmids containing murine p53 or SV40 large T-antigen to ensure that they did not activate the reporter gene without a specific interacting partner. Expression of the fusion proteins in transformant yeast strains was confirmed by Western analysis using anti-Myc and -HA antibodies. The interaction was quantified by liquid β-galactosidase assay using O-nitrophenyl β-D-galactopyranoside as the substrate and was expressed in Miller units.

References

Asleson, C.M., and P.A. Lefebvre. 1998. Genetic analysis of flagellar length control in *Chlamydomonas reinhardtii*: a new long-flagella locus and extragenic suppressor mutations. *Genetics*. 148:693–702.

Barsel, S.E., D.E. Wexler, and P.A. Lefebvre. 1988. Genetic analysis of long-flagella mutants of *Chlamydomonas reinhardtii*. *Genetics*. 118:637–648.

Bengs, F., A. Scholz, D. Kuhn, and M. Wiese. 2005. LmxMPK9, a mitogen-activated protein kinase homologue affects flagellar length in *Leishmania mexicana*. *Mol. Microbiol*. 55:1606–1615.

Berman, S.A., N.F. Wilson, N.A. Haas, and P.A. Lefebvre. 2003. A novel MAP kinase regulates flagellar length in *Chlamydomonas*. *Curr. Biol*. 13:1145–1149.

Besset, V., K. Rhee, and D.J. Wolgemuth. 1999. The cellular distribution and kinase activity of the cdk family member Pctaire1 in the adult mouse brain and testis suggest functions in differentiation. *Cell Growth Differ*. 10:173–181.

Bisova, K., D.M. Krylov, and J.G. Umen. 2005. Genome-wide annotation and expression profiling of cell cycle regulatory genes in *Chlamydomonas reinhardtii*. *Plant Physiol*. 137:475–491.

Bradley, B.A., and L.M. Quarmby. 2005. A NIMA-related kinase, Cnk2p, regulates both flagellar length and cell size in *Chlamydomonas*. *J. Cell Sci*. 118:3317–3326.

Burns, R.G. 1973. Kinetics of the regeneration of sea-urchin cilia. *J. Cell Sci*. 13:55–67.

Chao W.S., M.D. Serpe, Y. Jia, W.L. Shelver, J.V. Anderson, and M. Umeda. 2007. Potential roles for autophosphorylation, kinase activity, and abundance of a CDK-activating kinase (Ee;CDKF1) during growth in leafy spurge. *Plant Mol. Biol*. 63:365–379.

Clary-Meinesz, C., J. Mouroux, P. Huitorel, J. Cosson, D. Schoevaert, and B. Blaive. 1997. Ciliary beat frequency in human bronchi and bronchioles. *Chest*. 111:692–697.

Cole, D.G., D.R. Diener, A.L. Himelblau, P.L. Beech, J.C. Fuster, and J.L. Rosenbaum. 1998. *Chlamydomonas* kinesin-II-dependent intraflagellar transport (IFT): IFT particles contain proteins required for ciliary assembly in *Caenorhabditis elegans* sensory neurons. *J. Cell Biol*. 141:993–1008.

Davenport, J.R., and B.K. Yoder. 2005. An incredible decade for the primary cilium: a look at a once-forgotten organelle. *Am. J. Physiol. Renal Physiol*. 289:F1159–F1169.

Debuchy, R., S. Purton, and J.D. Rochaix. 1989. The argininosuccinate lyase gene of *Chlamydomonas reinhardtii*: an important tool for nuclear transformation and for correlating the genetic and molecular maps of the ARG7 locus. *EMBO J*. 8:2803–2809.

Dentler, W. 2005. Intraflagellar transport (IFT) during assembly and disassembly of *Chlamydomonas* flagella. *J. Cell Biol*. 170:649–659.

Devault, A., A.M. Martinez, D. Fesquet, J.C. Labbe, N. Morin, J.P. Tassan, E.A. Nigg, J.C. Cavadore, and M. Doree. 1995. MAT1 ('menage a trois') a new RING finger protein subunit stabilizing cyclin H-cdk7 complexes in starfish and *Xenopus* CAK. *EMBO J*. 14:5027–5036.

Fischer, N., and J.D. Rochaix. 2001. The flanking regions of PsaD drive efficient gene expression in the nucleus of the green alga *Chlamydomonas reinhardtii*. *Mol. Genet. Genomics*. 265:888–894.

Gibbs, C.S., and M.J. Zoller. 1991. Rational scanning mutagenesis of a protein kinase identifies functional regions involved in catalysis and substrate interactions. *J. Biol. Chem*. 266:8923–8931.

Hemmer, W., M. McGlone, I. Tsigelny, and S.S. Taylor. 1997. Role of the glycine triad in the ATP-binding site of cAMP-dependent protein kinase. *J. Biol. Chem*. 272:16946–16954.

Hou, Y., G.J. Pazour, and G.B. Witman. 2004. A dynein light intermediate chain, D1bLIC, is required for retrograde intraflagellar transport. *Mol. Biol. Cell*. 15:4382–4394.

Huang, B.Q., T.V. Masyuk, M.A. Muff, P.S. Tietz, A.I. Masyuk, and N.F. Larusso. 2006. Isolation and characterization of cholangiocyte primary cilia. *Am. J. Physiol. Gastrointest. Liver Physiol*. 291:G500–G509.

Huangfu, D., A. Liu, A.S. Rakeman, N.S. Murcia, L. Niswander, and K.V. Anderson. 2003. Hedgehog signalling in the mouse requires intraflagellar transport proteins. *Nature*. 426:83–87.

Iomini, C., V. Babaev-Khaimov, M. Sassaroli, and G. Piperno. 2001. Protein particles in *Chlamydomonas* flagella undergo a transport cycle consisting of four phases. *J. Cell Biol*. 153:13–24.

Jekely, G., and D. Arendt. 2006. Evolution of intraflagellar transport from coated vesicles and autogenous origin of the eukaryotic cilium. *Bioessays*. 28:191–198.

Kano, F., A.R. Tanaka, S. Yamauchi, H. Kondo, and M. Murata. 2004. Cdc2 kinase-dependent disassembly of endoplasmic reticulum (ER) exit sites inhibits ER-to-Golgi vesicular transport during mitosis. *Mol. Biol. Cell*. 15:4289–4298.

Kozminski, K.G., K.A. Johnson, P. Forscher, and J.L. Rosenbaum. 1993. A motility in the eukaryotic flagellum unrelated to flagellar beating. *Proc. Natl. Acad. Sci. USA*. 90:5519–5523.

Lees, E.M., and E. Harlow. 1993. Sequences within the conserved cyclin box of human cyclin A are sufficient for binding to and activation of cdc2 kinase. *Mol. Cell. Biol*. 13:1194–1201.

Lefebvre, P.A., C.D. Silflow, E.D. Wieben, and J.L. Rosenbaum. 1980. Increased levels of mRNAs for tubulin and other flagellar proteins after amputation or shortening of *Chlamydomonas* flagella. *Cell*. 20:469–477.

Liu, Y., C. Wu, and K. Galaktionov. 2004. p42, a novel cyclin-dependent kinase-activating kinase in mammalian cells. *J. Biol. Chem.* 279:4507–4514.

Lowe, M., C. Rabouille, N. Nakamura, R. Watson, M. Jackman, E. Jamsa, D. Rahman, D.J. Pappin, and G. Warren. 1998. Cdc2 kinase directly phosphorylates the cis-Golgi matrix protein GM130 and is required for Golgi fragmentation in mitosis. *Cell*. 94:783–793.

Loyer, P., J.H. Trembley, R. Katona, V.J. Kidd, and J.M. Lahti. 2005. Role of CDK/cyclin complexes in transcription and RNA splicing. *Cell. Signal.* 17:1033–1051.

Marshall, W.F., and J.L. Rosenbaum. 2001. Intraflagellar transport balances continuous turnover of outer doublet microtubules: implications for flagellar length control. *J. Cell Biol.* 155:405–414.

Mayfield, S.P., P. Bennoun, and J.D. Rochaix. 1987. Expression of the nuclear encoded OEE1 protein is required for oxygen evolution and stability of photosystem II particles in *Chlamydomonas reinhardtii. EMBO J.* 6:313–318.

McVittie, A. 1972. Flagellum mutants of *Chlamydomonas reinhardtii. J. Gen. Microbiol.* 71:525–540.

Morgan, D.O. 1997. Cyclin-dependent kinases: engines, clocks, and microprocessors. *Annu. Rev. Cell Dev. Biol.* 13:261–291.

Nebreda, A.R. 2006. CDK activation by non-cyclin proteins. *Curr. Opin. Cell Biol.* 18:192–198.

Nguyen, R.L., L.-W. Tam, and P.A. Lefebvre. 2005. The *LF1* gene of *Chlamydomonas reinhardtii* encodes a novel protein required for flagellar length control. *Genetics*. 169:1415–1424.

Niggemann, B., A. Muller, A. Nolte, N. Schnoy, and U. Wahn. 1992. Abnormal length of cilia–a cause of primary ciliary dyskinesia–a case report. *Eur. J. Pediatr.* 151:73–75.

Palmer, K.J., J.E. Konkel, and D.J. Stephens. 2005. PCTAIRE protein kinases interact directly with the COPII complex and modulate secretory cargo transport. *J. Cell Sci.* 118:3839–3847.

Pan, J., and W.J. Snell. 2005. *Chlamydomonas* shortens its flagella by activating axonemal disassembly, stimulating IFT particle trafficking, and blocking anterograde cargo loading. *Dev. Cell*. 9:431–438.

Pan, J., Q. Wang, and W.J. Snell. 2004. An aurora kinase is essential for flagellar disassembly in *Chlamydomonas. Dev. Cell*. 6:445–451.

Pazour, G.J., C.G. Wilkerson, and G.B. Witman. 1998. A dynein light chain is essential for the retrograde particle movement of intraflagellar transport (IFT). *J. Cell Biol.* 141:979–992.

Pedersen, L.B., M.S. Miller, S. Geimer, J.M. Leitch, J.L. Rosenbaum, and D.G. Cole. 2005. *Chlamydomonas* IFT172 is encoded by FLA11, interacts with CrEB1, and regulates IFT at the flagellar tip. *Curr. Biol.* 15:262–266.

Piperno, G., E. Siuda, S. Henderson, M. Segil, H. Vaananen, and M. Sassaroli. 1998. Distinct mutants of retrograde intraflagellar transport (IFT) share similar morphological and molecular defects. *J. Cell Biol.* 143:1591–1601.

Qin, H., D.R. Diener, S. Geimer, D.G. Cole, and J.L. Rosenbaum. 2004. Intraflagellar transport (IFT) cargo: IFT transports flagellar precursors to the tip and turnover products to the cell body. *J. Cell Biol.* 164:255–266.

Qin, H., D.T. Burnette, Y.K. Bae, P. Forscher, M.M. Barr, and J.L. Rosenbaum. 2005. Intraflagellar transport is required for the vectorial movement of TRPV channels in the ciliary membrane. *Curr. Biol.* 15:1695–1699.

Rascle, A., R.S. Stowers, D. Garza, J.A. Lepesant, and D.S. Hogness. 2003. L63, the *Drosophila* PFTAIRE, interacts with two novel proteins unrelated to cyclins. *Mech. Dev.* 120:617–628.

Robinson, M.J., P.C. Harkins, J. Zhang, R. Baer, J.W. Haycock, M.H. Cobb, and E.J. Goldsmith. 1996. Mutation of position 52 in ERK2 creates a nonproductive binding mode for adenosine 5′-triphosphate. *Biochemistry*. 35:5641–5646.

Rosenbaum, J.L., J.E. Moulder, and D.L. Ringo. 1969. Flagellar elongation and shortening in *Chlamydomonas*. The use of cycloheximide and colchicine to study the synthesis and assembly of flagellar proteins. *J. Cell Biol.* 41:600–619.

Smith, D.S., and L.H. Tsai. 2002. Cdk5 behind the wheel: a role in trafficking and transport? *Trends Cell Biol.* 12:28–36.

Smith, L.A., N.O. Bukanov, H. Husson, R.J. Russo, T.C. Barry, A.L. Taylor, D.R. Beier, and O. Ibraghimov-Beskrovnaya. 2006. Development of polycystic kidney disease in juvenile cystic kidney mice: insights into pathogenesis, ciliary abnormalities, and common features with human disease. *J. Am. Soc. Nephrol.* 17:2821–2831.

Snyder, M.A., J.M. Bishop, J.P. McGrath, and A.D. Levinson. 1985. A mutation at the ATP-binding site of pp60v-src abolishes kinase activity, transformation, and tumorigenicity. *Mol. Cell. Biol.* 5:1772–1779.

Song, L., and W.L. Dentler. 2001. Flagellar protein dynamics in *Chlamydomonas. J. Biol. Chem.* 276:29754–29763.

Tam, L.-W., and P.A. Lefebvre. 1993. Cloning of flagellar genes in *Chlamydomonas reinhardtii* by DNA insertional mutagenesis. *Genetics*. 135:375–384.

Tam, L.-W., W.L. Dentler, and P.A. Lefebvre. 2003. Defective flagellar assembly and length regulation in *LF3* null mutants in *Chlamydomonas. J. Cell Biol.* 163:597–607.

Tarricone, C., R. Dhavan, J. Peng, L.B. Areces, L.H. Tsai, and A. Musacchio. 2001. Structure and regulation of the CDK5-p25(nck5a) complex. *Mol. Cell.* 8:657–669.

Ubersax, J.A., E.L. Woodbury, P.N. Quang, M. Paraz, J.D. Blethrow, K. Shah, K.M. Shokat, and D.O. Morgan. 2003. Targets of the cyclin-dependent kinase Cdk1. *Nature*. 425:859–864.

Wang, Q., J. Pan, and W.J. Snell. 2006. Intraflagellar transport particles participate directly in cilium-generated signaling in *Chlamydomonas. Cell*. 125:549–562.

Wilson, N.F., and P.A. Lefebvre. 2004. Regulation of flagellar assembly by glycogen synthase kinase 3 in *Chlamydomonas reinhardtii. Eukaryot. Cell*. 3:1307–1319.

Wohlbold, L., S. Larochelle, J.C. Liao, G. Livshits, J. Singer, K.M. Shokat, and R.P. Fisher. 2006. The cyclin-dependent kinase (CDK) family member PNQALRE/CCRK supports cell proliferation but has no intrinsic CDK-activating kinase (CAK) activity. *Cell Cycle*. 5:546–554.

Xu, B., J.M. English, J.L. Wilsbacher, S. Stippec, E.J. Goldsmith, and M.H. Cobb. 2000. WNK1, a novel mammalian serine/threonine protein kinase lacking the catalytic lysine in subdomain II. *J. Biol. Chem.* 275:16795–16801.

Yankulov, K.Y., and D.L. Bentley. 1997. Regulation of CDK7 substrate specificity by MAT1 and TFIIH. *EMBO J.* 16:1638–1646.

Yoshikawa, S., J.L. Bonkowsky, M. Kokel, S. Shyn, and J.B. Thomas. 2001. The derailed guidance receptor does not require kinase activity in vivo. *J. Neurosci.* 21:RC119.